

Integration of polymer and metal microstructures using liquid-phase photopolymerization

Abhishek K Agarwal¹, David J Beebe² and Hongrui Jiang¹

¹ Department of Electrical and Computer Engineering, University of Wisconsin-Madison, 1415 Engineering Drive, Madison, WI 53706, USA

² Department of Biomedical Engineering, University of Wisconsin-Madison, 1550 Engineering Drive, Madison, WI 53706, USA

E-mail: hongrui@engr.wisc.edu

Received 6 August 2005, in final form 15 December 2005

Published 9 January 2006

Online at stacks.iop.org/JMM/16/332

Abstract

In this paper we demonstrate, using a fabrication technique, liquid-phase photopolymerization (LP³) for the relatively fast and low-cost integration of thick polymers and electroformed metal microstructures to develop a range of microfluidic components and systems. Liquid-phase UV-photosensitive polymers, similar to negative-tone photoresists, are used to create both polymer microstructures and molds to define electroformed metal (here, nickel—Ni) microstructures. This fabrication process can act as a stand-alone or appended one; it is gentle to allow processing after a metal structure has been released since fabrication occurs only at designated areas on a substrate, i.e. no spinning/casting of photosensitive materials, and self-planarization is achieved since photopolymerization of polymers occurs in the liquid phase. Photopatterned polymer and electroformed Ni microstructures are fabricated using LP³ with a low-end (low-cost) lithographic system. A variety of functional microfluidic components and systems, e.g., an active and a passive chaotic micromixer, and gear trains, are fabricated by utilizing a sequential step-and-repeat LP³ process to demonstrate the integration of polymers and metals.

(Some figures in this article are in colour only in the electronic version)

1. Introduction

Polymers have been used extensively in the miniaturization of lab-on-a-chip systems to develop a range of devices and complex 3D multi-layer structures [1–7], many of which are applied in microfluidic handling and manipulation, optics, micromechanics, sensors/actuators, chemical and bio-medical fields [8, 9]. Similarly, metal structures are also important in microfabrication serving as electrical conduits, and (thick) structural and integral (released) components [10–13]. However, many of the existing fabrication techniques do not readily permit cross-platform integration of high-aspect ratio polymers and metals, and may require final assembly of components built from different platforms [14–16]. Furthermore, the processing often necessitates clean room

environments and costly lithographic equipment, and involves long and sometimes harsh (chemical) polymer-defining processing steps. For example, many of the techniques for thick metal patterning, such as LIGA (lithografie galvanofornung abformung) [17–20], sacrificial metallic mold [21, 22], ultraviolet (UV)-LIGA [23, 24], deep reactive ion etch [25] and excimer laser [2, 26] impose high costs and long polymer definition times. Likewise, photopatterning of polymer structures often requires either long deposition times or spin-coating, which can be difficult to undertake on substrates with released microstructures.

Consequently, we present an alternative and lower cost option that exploits a fabrication technique, liquid-phase photopolymerization (LP³) [27–29], to facilitate integration of polymer and metal microstructures. Previous research

using LP³ has demonstrated a variety of microfluidic devices and components outside the clean room [27, 30]. We have previously used this relatively rapid and low-cost fabrication process to construct nickel (Ni) rotors in microfluidic channels for microfluidic devices [28, 29, 31, 32]. It was demonstrated that the fabrication process can act as a stand-alone or appended one and allow for a wide variety of substrates, including silicon, silicon nitride/oxide and glass [28], providing increased compatibility with integrated circuit (IC)-based MEMS processing.

In this paper, specific fabricated examples help demonstrate additional advantages offered by this fabrication technique to facilitate integration of thick polymer and metal microstructures. We first demonstrate that LP³ of photosensitive polymers enables rapid prototyping and patterning of thick polymer structures, often in a matter of minutes. Second, we show that these same polymers can also be utilized as molds for the electroforming of metal (here, Ni) microstructures. Finally, by employing a sequential step-and-repeat LP³ process, the remaining three sections illustrate the flexibility and versatility of this fabrication technique: (1) integration of polymer and metal microstructures by fabricating an active micromixer, (2) since photopolymerization occurs in the liquid phase, it allows for self-planarization on substrates with varying (3D) topography, and (3) because the process is gentle to be used on substrates with released structures and requires no spinning/casting of photosensitive materials, multi-layer devices and designated area processing on substrates with already-released microstructures can be realized.

2. Polymer photopatterning and Ni electroforming process

The fabrication process described here leverages advantages from LP³ to form thick planar two-dimensional polymer microstructures cast into the z -direction (3D) that also afford the capability of acting as molds for Ni electroplating. The photomask transfers a two-dimensional negative pattern to the photosensitive polymer. Because of the polymer thickness, a die-cast form of the pattern emerges.

A brief description of the photosensitive polymer and lithography setup is provided first. The general polymer photopatterning and Ni electroplating process are discussed next. The process is characterized by imaging polymer spaces and the resulting Ni lines of varying thicknesses and widths.

2.1. Photosensitive polymer and lithography setup

A photosensitive polymer, similar to negative-tone photoresists, is used here to pattern the polymer structures, and molds (for subsequent Ni electroplating). The photosensitive polymer consists of three constituents in the following weight ratios: 31.66:1.66:1.0 \rightarrow monomer—*isobornyl acrylate* (IBA, Surface Specialties UCB, Smyrna, GA, USA), crosslinker—*tetraethylene glycol dimethacrylate* (TeGDMA, Sigma-Aldrich, St Louis, MO, USA) and photoinitiator—*2,2-dimethoxy-2-phenylacetophenone* (DMPA, Sigma-Aldrich, St Louis, MO, USA). The three materials are mixed together in a glass vial using a sonicator. Exposure to a UV light

source (365 nm) causes the pre-polymer solution to harden (poly(IBA)).

Photolithography is accomplished by using a low-cost (under 6500 USD) desktop EXFO Acticure 4000 (EXFO Photonic Solutions, Inc., Mississauga, Ontario, Canada) UV light source (365 nm) with a spot-diameter focusing/collimation lens attached at the output of the lightguide. To minimize effects of varying UV intensity across the 6.35 cm diameter UV spot beam, devices were placed on a rotating stage and continuously rotated manually during exposure. The separation distance between the device/photomask and spot-diameter focus/collimation lens is 20.3 cm. The fabrication process is scalable to higher quality (and, consequently, higher cost) lithography systems if dictated by the final application(s). High resolution (3600 dpi) film photomasks (Silverline Studio, Madison, WI, USA) are used to transfer patterns to the photosensitive polymer.

2.2. General polymer photopatterning

Pre-cleaned microscope glass slides (76.2 mm \times 25.4 mm \times 1.0 mm, Fisher Scientific, Pittsburgh, PA, USA) are used as substrates. As an example, the negative-image mold of the letter 'W' is photopatterned. Figure 1 shows the general polymer fabrication process, which takes less than 10 min for polymer definition and 15 min for a post-development softbake.

Cavities are created between the glass slide and film photomask using 125 μm thick double-sided adhesive tape (figure 1(a)). Although, in this example, a 250 μm thick cavity was created, thicknesses of 125 and 375 μm were also studied in this paper. The IBA-based pre-polymer is squeezed into the cavity through one of the filling ports using transfer pipettes (figure 1(a)). It is photopatterned by UV exposure (intensity, $I_{\text{UV}} = 7.7 \text{ mW cm}^{-2}$; time, $t_{250 \mu\text{m}} = 19.5 \text{ s}$) to render a negative-image mold of the letter 'W'. The photomask is peeled off and the device is developed in a bath of 100% ethyl alcohol for 180–240 s. The development process rinses away the unpolymerized pre-polymer, leaving behind a hardened poly(IBA) mold of the letter 'W'. The device is softbaked on a hotplate at 50 $^{\circ}\text{C}$ for 15 min (figure 1(b)).

Polymer photopatterning was characterized by fabricating poly(IBA) spaces of three varying widths (increments of 12.5, 25.0 and 37.5 μm) in three respective poly(IBA) thicknesses—125, 250 and 375 μm . This allows analysis of the cross-section (sidewalls) of the photopatterned poly(IBA) structures. Polymer microstructures of varying thickness were fabricated by stacking an appropriate number of 125 μm thick double-sided adhesive tapes (figure 1(a)). The poly(IBA) spaces were photopatterned on glass slides using similar processing steps as outlined in figure 1: $t_{125 \mu\text{m}} = 16.5 \text{ s}$; $t_{250 \mu\text{m}} = 20.0 \text{ s}$; $t_{375 \mu\text{m}} = 23.5 \text{ s}$. As with many photoresists, poly(IBA) can also be polymerized in a small range of varying exposure times and intensities.

The devices were sputtered with a thin layer of Cr (~ 70 – 100 \AA) using a CVC 601 dc sputterer to prepare the devices for SEM imaging (JEOL JSM 6100, Materials Science Center, University of Wisconsin-Madison). Figure 2 shows an example perspective-view SEM image of a photopatterned poly(IBA) spaces (250 μm thick). The obtained SEM image

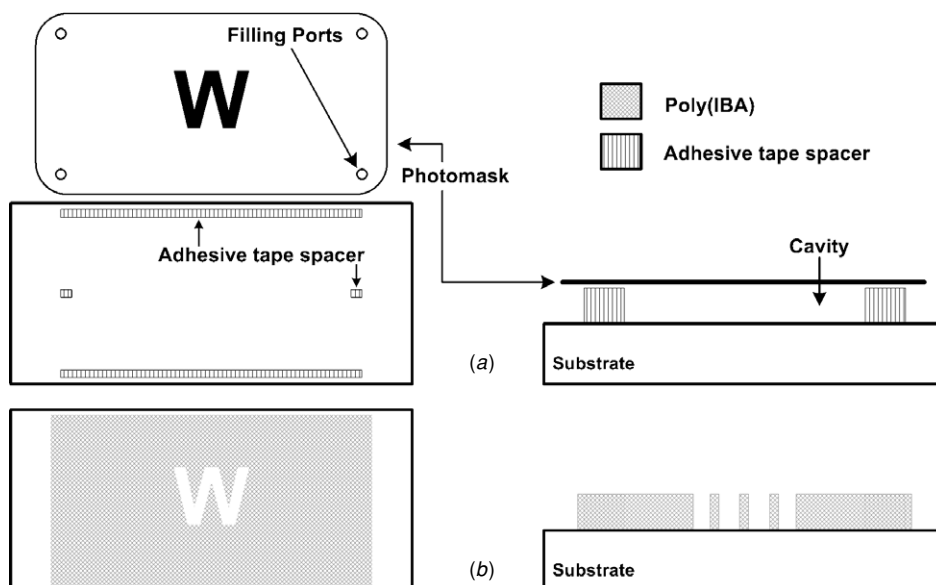


Figure 1. General liquid-phase photopolymerization polymer fabrication (top view on left; cross-section on right) to fabricate poly(IBA)-based microstructures. Here, the letter ‘W’ is photopatterned. (a) A 250 μm cavity is created between the microscope glass slide substrate and film photomask. The cavity is filled with the IBA-based pre-polymer. (b) The pattern is transferred to the polymer upon exposure to UV light. This results in the negative-image mold of the letter ‘W’.

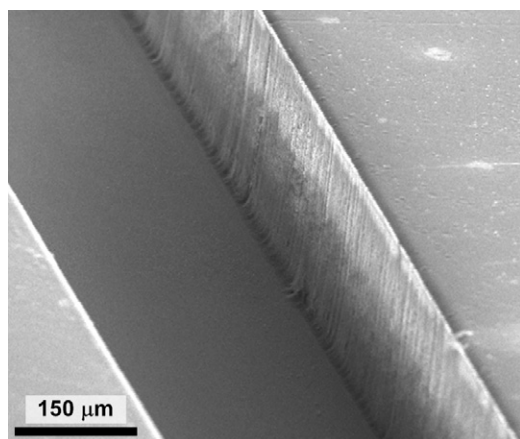


Figure 2. Example SEM image of a photopatterned poly(IBA) space showing the resulting sidewall. The poly(IBA) thickness and space width, as photopatterned, are 250 μm and 400 μm , respectively.

shows that the space assumes a slightly re-entrant (overcut) shape for thicker poly(IBA) molds. The sidewall profiles of the resulting Ni lines shown later in figure 5 further support this observation. Visual observation under a stereo microscope showed the minimum line space widths that could be photopatterned in 125, 250 and 375 μm thick poly(IBA) molds were 137.5, 175 and 187.5 μm , respectively. These photopatterning features are imposed by the limitations of the photomask resolution and UV exposure system (e.g. scattering and reflectance) used here. Polymer overcut shapes have also been observed with many other negative-tone photoresist processing; similarly, here too there are trade-offs between fine line widths, sidewall profiles and complete exposure/polymerization [33]. Fine-tuning the polymerization process, e.g., UV intensity and time exposure, and increasing the collimation of the current UV source may

aid in obtaining straighter sidewalls for thicker poly(IBA) molds [34].

2.3. General Ni electroforming process

Poly(IBA) molds photopatterned using LP³ can also work to define the active sites for Ni microstructure electroforming. As an example, the process is adapted from the example in figure 1 to fabricate a 3D Ni structure of the letter ‘W’. The photopatterning of the poly(IBA) mold takes place on glass slides previously coated with thin layers of Ti/Cu/Ti (0.06/0.30/0.06 μm) using a CVC 601 dc sputterer. The bottom and top Ti layers serve to promote adhesion to the glass slide and prevent oxidation of the middle Cu layer, respectively. The Cu layer serves as the future seed layer for Ni electroplating. Figure 3 shows the general Ni electroforming process.

Once the negative-image mold of the letter ‘W’ is photopatterned (figure 3(a)) on the Ti/Cu/Ti coated glass slide using the steps prescribed in figure 1, the device is prepared for Ni electroplating at the active sites, i.e., where no poly(IBA) exists. The exposed top Ti layer is removed using a 1:10 mixture of HF:H₂O (HF—technical grade, 48–50%, Fisher Scientific, Fairlawn, NJ, USA). See figure 3(b). The Ni electroplating bath, agitated at a constant 200 rpm, consists of 1:0.01 Microfab NI 100 make-up solution and Microfab NI 100 wetting agent (Enthone-OMI, West Haven, CT, USA). The plating solution pH is between 2.75 and 4.5 [35]. The bath temperature, maintained at a temperature of 50 ± 1 °C, is continuously monitored by a type-K thermocouple probe. High purity Ni gauze (no. 39704, Alfa Aesar, Ward Hill, MA, USA) is used as the Ni source (anode) for electroplating. Ni is electroplated onto the active sites on the glass slide (cathode; where Cu is exposed) at a rate of approximately 0.60–1.00 $\mu\text{m min}^{-1}$ using a current density of 5×10^{-4} A mm^{-2}

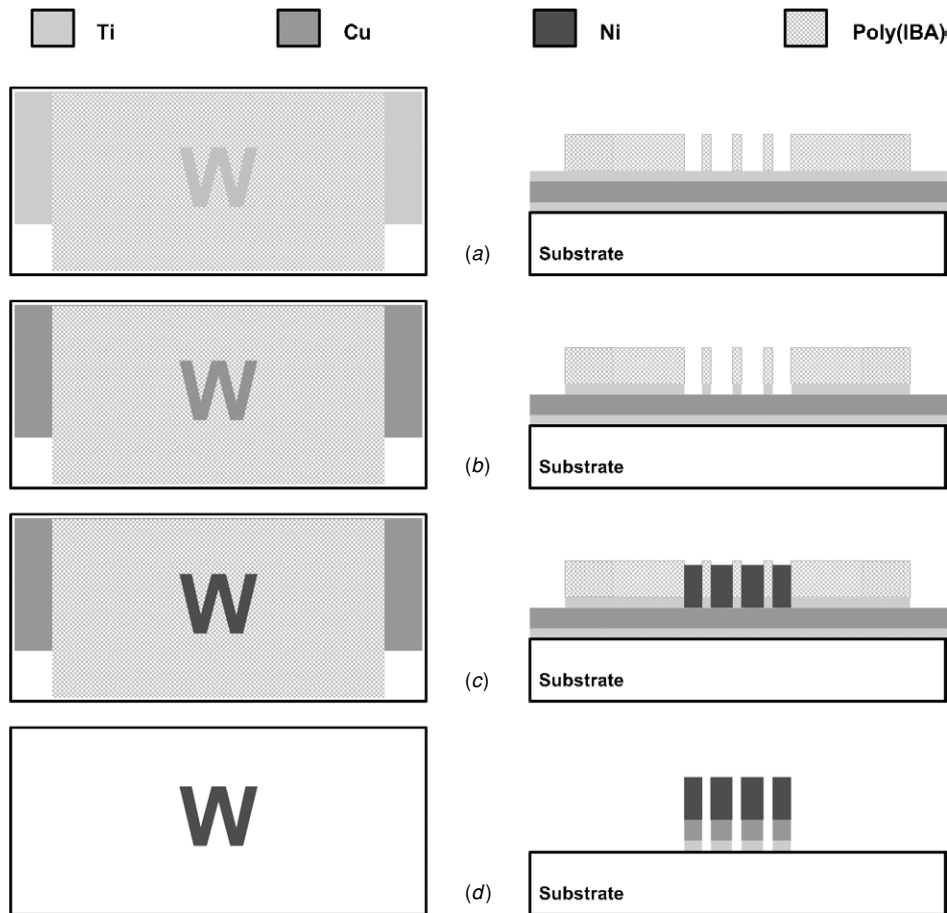


Figure 3. General liquid-phase photopolymerization fabrication process for electroforming Ni structures (top view on left; cross-section on right). Continued from figure 1, the letter ‘W’ is electroformed. (a) The negative-image poly(IBA) mold is fabricated on a glass slide coated with (Ti/Cu/Ti). (b) The top Ti layer is removed to expose the underlying Cu layer. (c) With the poly(IBA) serving as a mold, Ni electroplating is performed at the active sites. (d) The poly(IBA) mold and exposed seed metal layers are removed, leaving behind the die-casted three-dimensional Ni structure of the letter ‘W’.

[35]. Given this range of deposition rate, this specific electroplating session took approximately 120 min (figure 3(c)).

Next, to decrease the adhesion of the poly(IBA) mold to the glass slide, the poly(IBA) mold and device are immersed in a bath of 3:1 methanol and acetone for several hours. The poly(IBA) mold is removed, leaving behind the Ni microstructure on the glass substrate. The exposed seed metal layers are also removed (figure 3(d)) using 1:10 HF:H₂O for Ti removal and 1:1:10 HAC:H₂O₂:H₂O (HAC—glacial HPLC grade, H₂O₂—30%; Fisher Scientific, Fairlawn, NJ, USA) for Cu removal [36]. Figure 4 shows a SEM image of the resulting letter ‘W’. The vertical ridges observed on the oblique sidewall of the letter ‘W’ structure are apparent because of the film photomask quality—all oblique lines on the film photomask were verified under a microscope to have a jagged line texture. As shown in section 3.1, this fabrication process also permits release of the Ni microstructure from the substrate by etching the underlying metal seed layers (Ti and/or Cu).

To observe the resulting sidewalls of Ni microstructures, this electroforming process was used to electroplate Ni lines on Ti/Cu/Ti coated microscope glass slides with the same three thicknesses and width increments dictated in section 2.2. Poly(IBA) molds of three thicknesses were photopatterned on

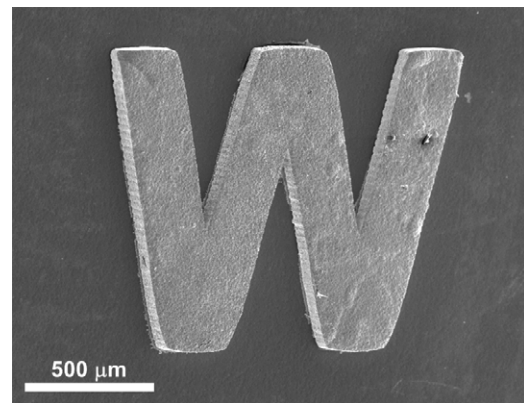


Figure 4. SEM image of the resulting Ni structure from figure 3—the letter ‘W’ (~100–125 μm thick). The electroplating mold was fabricated using liquid-phase photopolymerization.

glass substrates with the following time exposures: $t_{125\ \mu\text{m}} = 16.5\ \text{s}$, $t_{250\ \mu\text{m}} = 20.0\ \text{s}$ and $t_{375\ \mu\text{m}} = 23.5\ \text{s}$. SEM images of each Ni line thickness are shown in figures 5(a)–(c). The Ni lines assume straighter sidewalls as the thickness of the poly(IBA) mold decreases. A slight tapering of the profile in the z -direction is apparent from thick Ni line SEM

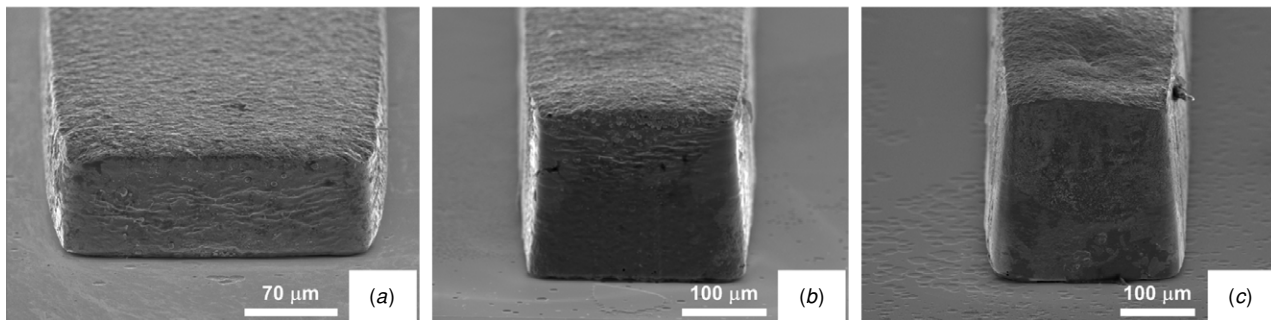


Figure 5. Electroplated Ni lines on microscope glass slide substrates. The line widths, as photopatterned, and poly(IBA) mold thicknesses are (a) 212.5 μm wide, 125 μm. (b) 225 μm wide, 250 μm. (c) 187.5 μm wide, 375 μm.

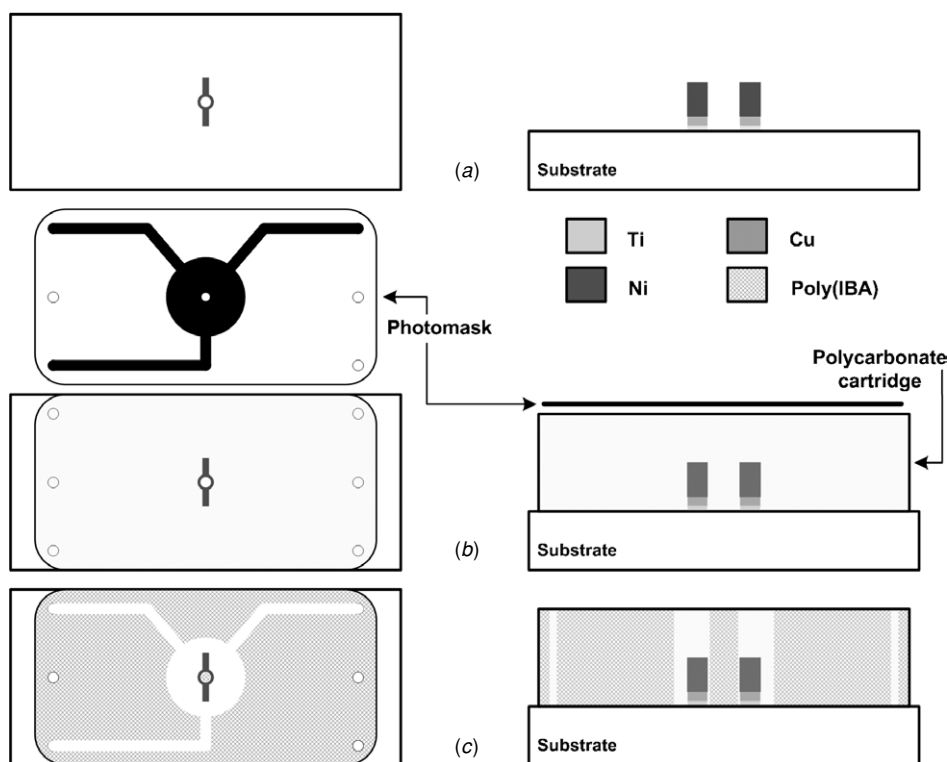


Figure 6. General liquid-phase photopolymerization (LP³) fabrication process for integrating metal and polymer structures (top view on left; cross-section on right). An example of an active micromixer is shown here. (a) A two-blade Ni rotor has been previously fabricated on a substrate. (b) A 250 μm thick polycarbonate cartridge is adhered to the substrate. The cartridge cavity is filled with the liquid pre-polymer mixture. The channels, mixing chamber and central post at the axis of the Ni rotor are photopatterned through the film photomask. (c) The unpolymerized pre-polymer is removed, resulting in an integrated polymer/metal active micromixer.

images, corresponding to the overcut profile observed for the poly(IBA) mold in figure 2.

3. Integration of polymer and Ni structures

Integration of polymer and metal (here, electroplated Ni) microstructures is accomplished by applying a sequential step-and-repeat LP³ process. This fabrication technique offers many benefits which are discussed in the following three sections.

3.1. Active micromixer

Fabrication of an active micromixer helps demonstrate the ability to integrate polymer and Ni structures. The micromixer,

fabricated on a glass slide, has an electroplated Ni rotor that rotates around a central axis poly(IBA) post. The fluid channels (two inputs and one output) and mixing chamber are fabricated from poly(IBA). Upon activation of an external rotating magnetic stirrer, the Ni rotor rotates in the *x*-*y* plane inside the mixing chamber and mixes the two input fluids. Figure 6 describes how the electroformed Ni rotor is to be integrated with a polymer-based central core post and microchannels to create an active micromixer.

Consider a two-blade Ni rotor that has been previously electroplated on a microscope glass slide using the aforementioned electroplating fabrication methods in figure 3. Once the poly(IBA) mold and seed metal layers have been removed (figure 6(a)), a 250 μm thick polycarbonate cartridge (HybriWells, Grace Bio-Labs, Inc., Bend, OR, USA) is placed

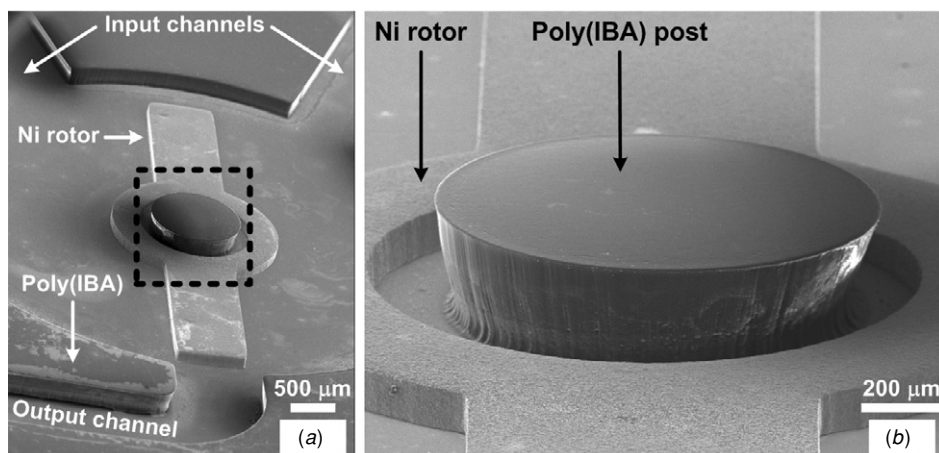


Figure 7. SEM images of a polymer and metal integrated device—an active micromixer—as fabricated in figure 6 using liquid-phase photopolymerization. (a) An overview SEM image of the active micromixer showing the two poly(IBA) input channels on the top, a Ni rotor with a central axis poly(IBA) post, and poly(IBA) output channel at the bottom. (b) The inset image (dashed black box in (a)) shows the central core poly(IBA) post photopatterned at the center axis of the Ni rotor.

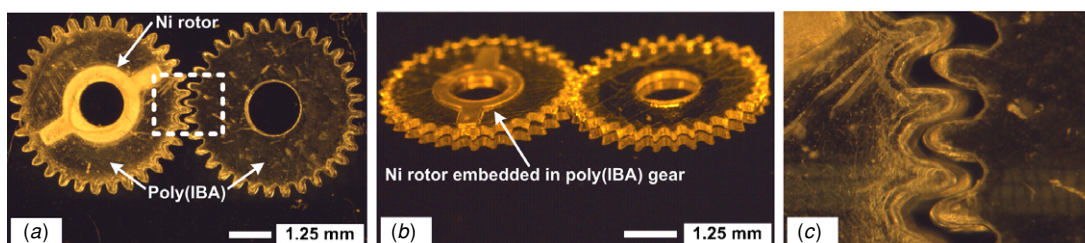


Figure 8. Optical photographs of a gear train fabricated using liquid-phase photopolymerization to demonstrate self-planarization. (a) A two-blade Ni rotor ($125\ \mu\text{m}$ thick) is embedded inside one poly(IBA) gear ($250\ \mu\text{m}$ thick), and subsequently engaged with another poly(IBA) gear. (b) A perspective photograph shows the self-planarization when embedding a Ni rotor inside a poly(IBA) gear. (c) The inset photograph (dashed white box in (a)) shows the gear teeth engaging with one another.

on top of the device to contain the Ni rotor (figure 6(b)). An adhesive gasket around the edge of the cartridge creates a pre-determined cavity thickness (125 , 250 , or $375\ \mu\text{m}$). The device is placed on a hotplate at $50\ ^\circ\text{C}$ for $5\ \text{min}$ to improve the adhesion of the gasket to the glass substrate. Once cool, the IBA-based pre-polymer solution is injected into the cartridge cavity. A film photomask is aligned on top of the cartridge and exposed to UV light ($I_{\text{UV}} = 7.7\ \text{mW cm}^{-2}$, $t_{250\ \mu\text{m}} = 20.5\ \text{s}$) to photopattern the microchannels, mixing chamber and central axis poly(IBA) post. A peristaltic pump is used in conjunction with 100% ethyl alcohol to remove the unpolymerized pre-polymer. The device is softbaked on a hotplate at $50\ ^\circ\text{C}$ for $15\ \text{min}$ (figure 6(c)). The last step (not shown here) is to release the Ni rotor from the glass substrate by etching the underlying Ti/Cu seed layers.

Prior to acquiring SEM images of the integrated micromixer, the adhesive polycarbonate cartridge is peeled off, and a thin layer of Cr is sputtered on the device. Figure 7(a) shows an SEM image of the two input channels on the top (width, $w = 1.0\ \text{mm}$), the Ni rotor ($w = 0.60\ \text{mm}$; length, $l = 2.0\ \text{mm}$; thickness, $\text{th} = 0.125\ \text{mm}$) with a central axis poly(IBA) post (diameter = $1.20\ \text{mm}$), and the output channel ($w = 1.0\ \text{mm}$) at the bottom. Figure 7(b) shows a close-up SEM image (dashed black box in figure 7(a)) of the electroformed Ni rotor integrated with a central axis poly(IBA) post.

3.2. Gear train—self-planarization

To demonstrate the self-planarization feature offered by LP³, a poly(IBA) gear train is constructed. One poly(IBA) gear is fabricated directly on top of an existing electroformed Ni rotor, while the other is fabricated directly on top of the substrate. Poly(IBA) posts are also photopatterned at the center axis of the gears. The embedded Ni rotor couples with an external rotating magnetic stirrer and rotates the individual poly(IBA) gear in the x - y plane. This causes the second poly(IBA) gear to rotate in the opposite direction.

A Ni rotor ($l/w/\text{th} = 1.0/0.35/0.125\ \text{mm}$) is first electroformed onto a glass slide substrate. The poly(IBA) gears (here, $\text{th} = 0.25\ \text{mm}$) and central axis posts can be photopatterned subsequently using a film photomask. The gear trains can be released by etching the underlying (sacrificial) Cu seed layer. Figure 8(a) shows a top-view image of the gear train with one gear containing the embedded Ni rotor. Note in figure 8(b) that LP³ helps realize self-planarization even when photopatterning on a thick electroformed Ni rotor since the polymerization step occurs in the liquid phase. Figure 8(c) shows a close-up optical image (dashed white box in figure 8(a)) of the gear train teeth engaged with one another. In addition to the benefit of photopatterning substrates with varying (3D) topography, this fabrication process also has potential to create multi-layer structures, one on top of the

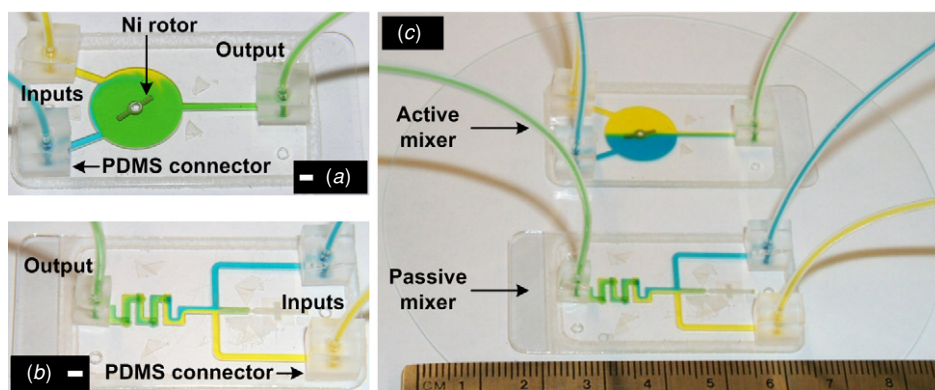


Figure 9. Optical images of an active micromixer (released Ni rotor) and two-layer passive chaotic micromixer constructed on the same 4 inch glass wafer to demonstrate designated area fabrication and post-release processing of multi-layer devices. Yellow- and blue-dyed water solutions are pumped through the channel networks. (a) An active micromixer with a released Ni rotor mixing two input fluids (external magnetic stirrer is activated). Scale bar—2.0 mm. (b) A two-layer passive chaotic micromixer. Scale bar—2.0 mm. (c) Complete device image showing both constructed micromixers.

other, again by employing a sequential step-and-repeat LP³ process (shown in section 3.3).

3.3. (Multi-layer) post-processing after Ni release

Spin-coating often suffers from the necessity to process the entire substrate, which can be complicated if structures on the substrate have already been released, as is often the case with MEMS processing. The LP³ fabrication technique, however, supports (multi-layer) processing after a structure has been released on a substrate because the process is gentle to released structures and does not require spin casting of photosensitive polymers, i.e., fabrication occurs only at designated areas on a substrate. This flexible advantage will be demonstrated in this paper via an example: a two-layer passive chaotic micromixer [37] will be fabricated on a 4 inch glass wafer which already houses a functional integrated active micromixer with a released Ni rotor (similar to the one developed in section 3.1). Fabrication of the active micromixer is similar to that prescribed in section 3.1, except that an already released two-blade Ni rotor is integrated with polymer structures to realize a functional active micromixer. This further demonstrates the flexibility of the fabrication technique to process released structures.

The released Ni rotor ($l/w/th = 2.0/0.60/0.20$ mm) is manually placed onto the surface of a 4 inch glass wafer and enclosed by a $375\ \mu\text{m}$ thick polycarbonate cartridge. After a 5 min softbake at $50\ ^\circ\text{C}$, the cartridge cavity is filled with the IBA-based pre-polymer solution, and a small magnet is used to position the released Ni rotor inside the cartridge. Once positioned, the poly(IBA) microchannels, mixing chamber, and central core post are photopatterned ($I_{UV} = 7.7\ \text{mW cm}^{-2}$, $t_{375\ \mu\text{m}} = 24.5$ s) in a single step through a film photomask similar to figure 6(b). Subsequent processing is the same as outlined in section 3.1. Poly(dimethylsiloxane) (PDMS) connectors are adhered to and aligned with three of the six filling ports (two inputs and one output) on the surface of the cartridge. Yellow- and blue-dyed water solutions are pumped through the channel network of the micromixer using a syringe pump. Since the external magnetic stirrer is on, the Ni rotor

rotates, mixing the two dyed water solutions into a green solution (figure 9(a)).

Next, a two-layer passive chaotic micromixer is constructed on the same 4 inch glass wafer. First, four small holes are punched at specific locations in a $250\ \mu\text{m}$ thick cartridge to allow fluid to flow between the two layers, thereby creating the 3D serpentine channel configuration. This cartridge is adhered to the glass wafer, filled with the IBA-based pre-polymer mixture and photopatterned through film photomask 1 ($I_{UV} = 7.7\ \text{mW cm}^{-2}$, $t_{375\ \mu\text{m}} = 21.0$ s). This first layer channel network is developed with 100% ethyl alcohol and softbaked at $50\ ^\circ\text{C}$ for 15 min. To create the second layer of this multi-layer micromixer, the first layer channel network is first filled with a green-dyed glycerin–water solution. This will prevent backflow of the IBA-based pre-polymer solution into the first layer when it is injected into the second cartridge cavity. Next, a second $250\ \mu\text{m}$ thick cartridge is aligned on top of the first, filled with the pre-polymer solution, and photopatterned similarly through film photomask 2 to form the connecting second layer channel network. PDMS connectors are also adhered to the two inputs and one output filling port. Yellow- and blue-dyed water solutions are subsequently pumped through the channel network using syringe pumps (figure 9(b)). Figure 9(c) shows the overall photograph of the 4 inch glass wafer housing both the active micromixer (with a released Ni rotor) and the two-layer passive chaotic micromixer. The LP³ fabrication process is gentle to allow post-fabrication of additional (multi-layer) components on the same wafer without undue stress on previously released devices.

4. Conclusion

The few fabrication methods that have realized successful integration of polymers and metals have often dictated expensive equipment, lengthy processing times and/or the use of different fabrication platforms. As an alternative, we have demonstrated the application of using LP³ to realize polymer microstructures and molds for Ni electroforming. The sequential application of the LP³ process allows (multi-layer) fabrication of integrated polymer

and metal microstructures. Here, fabricated examples of poly(IBA) and electroformed Ni microstructures, a polymer/Ni integrated active micromixer, Ni embedded gear trains, and a multi-layer chaotic micromixer alongside an already-released Ni rotor (part of an active micromixer, both on the same substrate) demonstrate the multitude of benefits of this fabrication technique: a gentle fabrication process, even to released structures on the substrate; fabrication of a device only occurs at designated areas, which allows (multi-layer) processing to occur even after a structure has been released; self-planarization, i.e., substrate topography is of little concern, since fabrication occurs in the liquid phase; and the ability to act as a stand-alone or appended process.

Merits of the fabrication process described here are low cost, fast turn around, and the capacity for integration. LP³ processing allows for a variety of resolutions that are, in essence, dictated by the application of the device. Therefore, the integration of the polymer and metal microstructures can be scaled to fit many applications. For example, if structures are of larger magnitude, the overall cost can be reduced further by using cheaper UV lithography systems. However, if applications require higher resolution microstructures, the lithography setup can be extended to a higher end (higher cost) system. Additionally, three-dimensional metal microstructures can be fabricated from corresponding three-dimensional polymer molds patterned using stereolithography, e.g., two-photon technology [38, 39]. Future studies are planned to optimize the polymerization process to realize both straighter sidewalls for thick polymer structures and a decrease in the minimum line feature that can be successfully photopatterned in poly(IBA).

Acknowledgments

This work is mainly supported by the Wisconsin Alumni Research Foundation (WARF) and partially by DARPA BioFlips program. The authors would like to thank the Wisconsin Center for Applied Microelectronics (WCAM) facility at the University of Wisconsin-Madison for clean room facilities. The authors are grateful to Richard Noll at the Materials Science Center at the University of Wisconsin-Madison for assistance in acquiring SEM images. The authors also recognize Tracy Drier (Chemistry GlassShop) at the University of Wisconsin-Madison for assistance in glass work. The authors thank Dr Liang Dong and Sudheer Sridharamurthy (University of Wisconsin-Madison) for technical discussions. The authors also acknowledge Thomas M Pearce (Washington University in St Louis, MO) and Dongshin Kim (University of Wisconsin-Madison) for assistance in film photomask design. The authors are grateful to the lab members in Professor David Beebe's research group (Microtechnology Medicine and Biology lab, University of Wisconsin-Madison).

References

- [1] Beebe D J, Moore J S, Bauer J M, Yu Q, Liu R H, Devadoss C and Jo B-H 2000 Functional hydrogel structures for autonomous flow control inside microfluidic channels *Nature* **404** 588–90
- [2] Eddington D T and Beebe D J 2004 Flow control with hydrogels *Adv. Drug Deliv. Rev.* **56** 199–210
- [3] Zou J, Wang X, Bullen D, Ryu K, Liu C and Mirkin C A 2004 A mould-and-transfer technology for fabricating scanning probe microscope probes *J. Micromech. Microeng.* **14** 204–11
- [4] Fan Z, Engel J M, Chen J and Liu C 2004 Parylene surface-micromachined membranes for sensor applications *J. Microelectromech. Syst.* **13** 484–90
- [5] Ryu K S, Shaikh K, Goluch E, Fan Z and Liu C 2004 Micro magnetic stir-bar mixer integrated with parylene microfluidic channels *Lab-on-a-Chip* **4** 608–13
- [6] Xie J, Shih J, Lin Q, Yang B and Tai Y-C 2004 Surface micromachined electrostatically actuated micro peristaltic pump *Lab-on-a-Chip* **4** 495–501
- [7] Agirregabiria M, Blanco F J, Berganzo J, Arroyo M T, Fullaondo A, Mayora K and Ruano-López J M 2005 Fabrication of SU-8 multilayer microstructures based on successive CMOS compatible adhesive bonding and releasing steps *Lab-on-a-Chip* **5** 542–52
- [8] de Mello A 2002 Plastic fantastic? *Lab-on-a-Chip* **2** 31N–6N
- [9] Yang H, Pan C-T and Chou M-C 2001 Ultra-fine machining tool/molds by LIGA technology *J. Micromech. Microeng.* **11** 94–9
- [10] Cohen A, Zhang G, Tseng F-G, Frodis U, Mansfeld F and Will P 1999 EFAB: rapid, low-cost desktop micromachining of high aspect ratio true 3-D MEMS *Proc. 12th IEEE Int. Conf. on MEMS (Orlando, FL, USA)* pp 244–51
- [11] Xie H, Erdmann L, Zhu X, Gabriel K J and Fedder G K 2002 Post-CMOS processing for high-aspect-ratio integrated silicon microstructures *J. Microelectromech. Syst.* **11** 93–101
- [12] Kim S-H, Lee S-H and Kim Y-K 2002 A high-aspect-ratio comb actuator using UV-LIGA surface micromachining and (110) silicon bulk micromachining *J. Micromech. Microeng.* **12** 128–35
- [13] Arnold D P, Cros F, Zana I, Veazie D R and Allen M G 2004 Electroplated metal microstructures embedded in fusion-bonded silicon: conductors and magnetic materials *J. Microelectromech. Syst.* **13** 791–8
- [14] Kovacs G T A 1998 *Micromachined Transducers Sourcebook* (New York: McGraw-Hill) pp 779–901
- [15] Mitchell P 2001 Microfluidics—downsizing large-scale biology *Nature Biotechnol.* **19** 717–21
- [16] Ehrnström R 2002 Miniaturization and integration: challenges and breakthroughs in microfluidics *Lab-on-a-Chip* **2** 26N–30N
- [17] Becker E W, Ehrfeld W, Hagmann P, Maner A and Munchmeyer D 1986 Fabrication of microstructures with high aspect ratios and great structural heights by synchrotron radiation lithography, galvanofforming, and plastic moulding (LIGA process) *Microelectron. Eng.* **4** 35–56
- [18] Guckel H 1998 High-aspect-ratio micromachining via deep x-ray lithography *Proc. IEEE* **86** 1586–93
- [19] Hruby J 2001 LIGA technologies and applications *MRS Bull.* **26** 337–40
- [20] Cheng C-M and Chen R-H 2004 Key issues in fabricating microstructures with high aspect ratios by using deep X-ray lithography *Microelectron. Eng.* **71** 335–42
- [21] Yoon J-B, Han C-H, Yoon E and Kim C-K 1999 Monolithic integration of 3-D electroplated microstructures with unlimited number of levels using planarization with a sacrificial metallic mold (PSMM) *Proc. IEEE Int. Conf. MEMS (Orlando, FL, USA)* pp 624–9
- [22] Choi Y-S, Yoon J-B, Kim B-I and Yoon E 2002 A high-performance MEMS transformer for silicon RF ICs *Proc. IEEE Int. Conf. MEMS (Las Vegas, NV, USA)* pp 653–6
- [23] Kukharenska E, Farooqui M M, Grigore L, Kraft M and Hollinshead N 2003 Electroplating moulds using dry film thick negative photoresists *J. Micromech. Microeng.* **13** S67–74

- [24] Ho C-H and Hsu W 2004 Experimental investigation of an embedded root method for stripping SU-8 photoresist in the UV-LIGA process *J. Micromech. Microeng.* **14** 356–64
- [25] Noell W, Clerc P-A, Jeanneret S, Hoogerwerf A, Niedermann P, Perret A and de Rooij N F 2004 MEMS for watches *Proc. IEEE MEMS (Maastricht, The Netherlands)* pp 1–4
- [26] Yang C-R, Hsieh Y-S, Hwang G-Y and Lee Y-D 2004 Photoablation characteristics of novel polyimides synthesized for high-aspect-ratio excimer laser LIGA process *J. Micromech. Microeng.* **14** 480–9
- [27] Beebe D J, Moore J S, Yu Q, Liu R H, Kraft M L, Jo B-H and Devadoss C 2000 Microfluidic tectonics: a comprehensive construction platform for microfluidic systems *Proc. Natl. Acad. Sci.* **97** 13488–93
- [28] Agarwal A K, Sridharamurthy S S, Pearce T M, Mensing G A, Beebe D J and Jiang H 2004 Magnetically-driven actuation using liquid-phase polymerization (LPP) and its application: a programmable mixer *Proc. Hilton Head: A Solid State Sensor, Actuator, and Microsystem Workshop (Hilton Head Island, SC, USA)* pp 121–4
- [29] Agarwal A K, Atencia J, Beebe D J and Jiang H 2004 Magnetically-driven temperature-controlled microfluidic actuators *Proc. 1st Int. Workshop on Networked Sensing System (Tokyo, Japan)* pp 51–5
- [30] Mensing G A, Pearce T and Beebe D J 2005 An ultra rapid method of creating 3D channels and microstructures *J. Assoc. Lab. Autom.* **10** 24–8
- [31] Agarwal A K, Sridharamurthy S S, Beebe D J and Jiang H 2005 Programmable autonomous micromixers and micropumps *J. Microelectromech. Syst.* **14** 1409–21
- [32] Agarwal A K, Sridharamurthy S S, Beebe D J and Jiang H 2005 An on-chip autonomous microfluidic cooling system *Proc. 13th Int. Conf. on Solid-State Sensors, Actuators, and Microsystems (Seoul, South Korea)* pp 364–7
- [33] Madou M 1997 *Fundamentals of Microfabrication* (New York: CRC Press) pp 5, 7, 13–4
- [34] Moorthy J, Mensing G A, Kim D, Mohanty S, Eddington D E, Tepp W H, Johnson E A and Beebe D J 2004 Microfluidic tectonics platform: a colorimetric, disposable botulinum toxin enzyme-linked immunosorbent assay system *Electrophoresis* **25** 1705–13
- [35] Microfab[®] NI 100 Data Sheet 2000 Enthone-OMI Inc., West Haven, CT, USA
- [36] Zou J, Liu C, Schutt-Aine J, Chen J and Kang S-M 2000 Development of a wide tuning range MEMS tunable capacitor for wireless communication systems *Proc. IEDM (San Francisco, CA, USA)* pp 403–6
- [37] Liu R H, Stremmer M A, Sharp K V, Olsen M G, Santiago J G, Adrian R J, Aref H and Beebe D J 2000 Passive mixing in a three-dimensional serpentine microchannel *J. Microelectromech. Syst.* **9** 190–7
- [38] Maruo S and Ikuta K 1999 Movable microstructures made by two-photon three-dimensional microfabrication *Proc. Int. Symp. Micromechatronics and Human Science (Nagoya, Japan)* pp 173–8
- [39] Zhang X, Jiang X N and Sun C 1999 Micro-stereolithography of polymeric and ceramic microstructures *Sensors Actuators A* **77** 149–56